Journal of Applied Polymer Science

Bulk Synthesis of Homogeneous and Transparent Bulk Core/Multishell Quantum Dots/PMMA Nanocomposites with Bright Luminescence

Yongsheng Ma,[1] Bingbo Zhang,[2] Mu Gu,[1] Shiming Huang,[1] Xiaolin Liu,[1] Bo Liu,[1] Chen Ni[1]

[1]Shanghai Key Laboratory of Special Artificial Microstructure Materials and Technology, Department of Physics, Tongji University, Shanghai 200092, People's Republic of China

[2]The Institute for Advanced Materials and Nano Biomedicine, Tongji University School of Medicine, Shanghai 200092, People's Republic of China

Correspondence to: M. Gu (E-mail: mgu@mail.tongji.edu.cn) or S. M. Huang (E-mail: smhuang2008@yahoo.com.cn).

ABSTRACT: Core/multishell CdSe/CdS/CdS/$Cd_{0.75}Zn_{0.25}S$/$Cd_{0.5}Zn_{0.5}S$/$Cd_{0.25}$ $Zn_{0.75}S$/ZnS/ZnS QDs/PMMA bulk nanocomposites were successfully synthesized. To achieve a homogeneous and stable dispersion in MMA monomers, QDs were first modified with amphiphilic polymer of poly(ethylene glycol)-oleate (PEG-oleate). Subsequently, the transparent and homogeneous bulk composites were obtained by photopolymerization. The TEM analysis of ultramicrotome cut of composite demonstrates that QDs are well dispersed in the PMMA matrix. UV–vis transmission spectra show the nanocomposites still maintain high transmittance even with QDs content of up to 6 wt %. The thermogravimetric analysis (TGA) reveals the incorporation of the QDs significantly improves the thermal stability of composites, as evidenced by the retardation of a degradation initiation by 60°C. Photoluminescence spectra suggest that the nanocomposites exhibit bright fluorescence under UV excitation. X-ray excited luminescence spectra show they have response to X-ray. All of the experimental results indicate the great promising applications of core/multishell QDs/PMMA nanocomposites in optical communication devices and radiation detectors. © 2013 Wiley Periodicals, Inc. J. Appl. Polym. Sci. 130: 1548–1553, 2013

KEYWORDS: photopolymerization; composites; optical properties; surfactants

Received 12 October 2012; accepted 17 March 2013; Published online 30 April 2013
DOI: 10.1002/app.39338

INTRODUCTION

Quantum dots (QDs) have been intensively studied in the past decades due to their unique, size-tunable optical and electronic properties, which are largely different from the bulk materials.[1,2] Therefore, they have show a great promise for many applications, such as thin film light-emitting devices,[3] nonlinear optical devices,[4] solar cells, biological labels,[5] and scintillation detection.[6–8] In our previous papers,[9–11] core/multishell QDs were prepared and shown the increased stability and quantum efficiency with respect to the plain core QDs.

To fabricate photonic and optoelectronic devices, QDs are usually incorporated into polymer matrix to maintain their functionalities as well as to improve their processability and has shown a great promise.[12–14] Moreover, the synergistic combination of QDs and polymer in nanocomposites may generate new properties which do not exist for either material alone. Among the wide variety of available polymers, poly(methyl methacrylate) (PMMA) possesses excellent properties such as exceptional optical clarity, good weather resistance, high mechanical strength, excellent dimensional stability, and resistance to laser damage, and has been a most extensively studied matrix for nanocomposites.[15–24]

Although the technology for incorporating QDs in thin polymeric film is extensively reported, stabilizing them into bulk polymer matrix with high contents remains a challenge.[15,17,25–27] The key issue for preparation of homogeneous and transparent nanocomposites is to disperse the QDs homogeneously into polymer without aggregation. A large number of complicated synthesis techniques have been developed to prevent phase separation during the polymerization process, including *in situ* formation of nanocrystals within monomer or polymer media,[28,29] incorporation of surface modified nanocrystals into polymer/monomer polymerized subsequently.[20,30–36] The former approach may produce undesired species in the host matrix, coming either from the products of the nanocrystals or synthesis process. In addition, a poor control on the nanocrystals size and the properties is another possible drawback of such approach. The mixing of prior synthesized nanocrystals with polymer results in extreme benefits. However, nanocrystals aggregation in polymer matrix must be avoided. Because of the variance of the nanocrytstals and polymer matrix, many researchers endeavored to develop proper

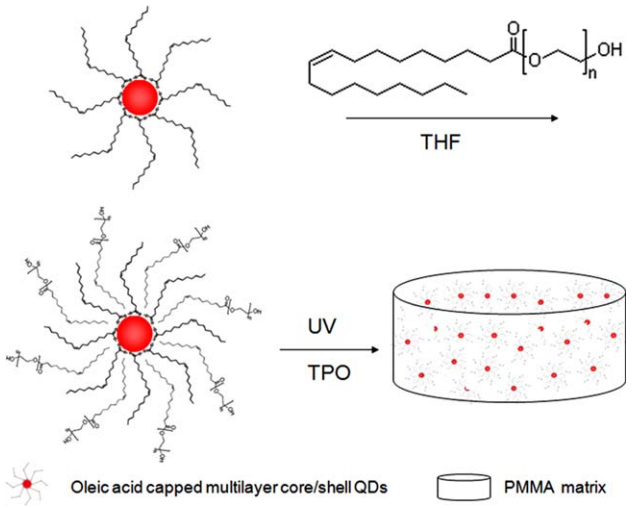

Scheme 1. *In situ* polymerization method for the generation of transparent QDs/PMMA nanocomposites. [Color figure can be viewed in the online issue, which is available at wileyonlinelibrary.com.]

surfactants and approaches to prevent phase separation. Zhang et al.[30] used a polymerizable surfactant octadecy-*p*-vinylbenzyldimethylammonium chloride (OVDAC) to transfer 3-mercaptocarboxylic acid stabilized QDs into monomer solution and polymerized to transparent bulk nanocomposites. Althues et al.[31] utilized the bulk polymerization of transparent dispersion containing ZnS:Mn nanocrystals in a mixture of methyl methacrylate (MMA) and acrylic acid (AA). Compared with water-soluble QDs, hydrophobic QDs, especially core/multishell QDs prepared through the nonhydrolytic solvent usually are of high quantum efficiency and an impressive control over nanoparticles shape and size.[37,38] However, relatively few studies have investigated on hydrophobic QDs/polymer bulk nanocomposites, especially using common poly(methyl methacrylate) (PMMA) as matrix.[20] The surfactant of amphiphilic polymer PEG-oleate has a long chain alkyl at one end interacting with the surface of QDs while PEG chains at the other end which is compatible with MMA monomer. Boyer et al.[22] employed this surfactant to render oleic acid coated $NaYF_4$ nanocrystals dispersible in MMA monomer and thus utilized thermal polymerization method for preparaction of transparent bulk $NaYF_4$/PMMA nanocomposites. Photopolymerization has advantages over thermal polymerization, such as rapid polymerization rate, low polymerization temperature, low energy consumption, easy process control, and has been widely use for polymerization of numerous acrylate monomers.[39]

Herein, a new simple and facile method of synthesis of a new QDs/PMMA nanocomposites is reported (Scheme 1), the obtained homogeneous nanocomposites maintain high transmittance even with 6 wt % solid content which is rarely reported before. And they exhibit bright luminescence under UV excitation and have response to X-ray, which suggests its promising applications in optical communication devices and scintillation detection.

EXPERIMENTAL

Materials

Cadmium oxide (99.5%), selenium power (99.99%), zinc oxide (99.9%), sulfur (99.98%), tri-*n*-octylphosphine oxide (TOPO, 90%), tributylphosphine (TOP, 90%), octadecylamine (ODA, 90%), oleic acid (OA, 90%), poly(ethylene glycol)-monooleate (M_n = 860) (PEG-oleate) were purchased from Aldrich, photoinitiator 2,4,6-trimethylbenzoyldiphenylphosphine oxide (TPO) were obtained from TCI. The aforementioned chemicals were used as received. Methyl methacrylate (MMA, 90 %) and tetrahydrofuran (THF) were purchased from Sinopharm Chemical Reagent and MMA was purified by distillation and stored at −20°C before use.

Synthesis of OA-Coated Core/Multishell QDs

In this article, CdSe/CdS/CdS/$Cd_{0.75}Zn_{0.25}S$/$Cd_{0.5}Zn_{0.5}S$/$Cd_{0.25}Zn_{0.75}S$/ZnS/ZnS (seven Layers) were synthesized according to a previously reported protocols.[9]

Synthesis of QDs-PMMA Bulk Nanocomposites

In a typical synthesis, the appropriate amounts of QDs were dispersed in THF in a 10 mL vial. Nearly 0.05–0.3 mL poly(ethylene glycol)-monooleate was added to the vial and ultrasonicated for 2 min, then the THF was removed under vacuum with a rotovap at 40°C. Then, 1 mL methyl methacrylate was added to the vial and the resulting dispersion was ultrasonicated for 30 min to obtain a clear dispersion. After photo initiator 2,4,6-trimethylbenzoyldiphenylphosphine oxide (TPO) (0.5 wt % of MMA, the molar ratio of monomer to photoinitiator is 692 : 1) was added, the mixture was ultrasonicated for 10 min to completely solve the photo initiator. The resulting clear dispersion was transferred to a vacuum drum degassing for 10 min. For thermal polymerization, the vial was placed into thermostatic water bath at 90°C for about 15 min, cooled to room temperature when the mixture reached certain viscosity. Then the vial was transferred into oven at 60°C and kept at this temperature for 24 h. For photopolymerization, the polymerization was initiated by placing the vial under a 300-W UV lamp for about 2 h when the nanocomposites became very rigid. Then the bulk composites were moved by breaking the glass vial and polished for optical measurement.

Characterization

X-ray diffraction (XRD) of the power samples was examined with a Bruker D8-Advance X-ray power diffractometer, with Cu Kα radiation (λ = 1.5418 Å). Transmission election microscope (TEM) was performed on QDs and composites using a JEOL 2010 transmission electron microscope operating at 200 kV. Samples for QDs were prepared by depositing a drop of the samples dispersed in different solvents onto a carbon-coated copper grid, the excess liquid was wicked away with filter paper, the solvent was evaporated at room temperature and the grid was dried in air. TEM measurements on the composite materials were performed by way of thin sections. The composite materials were first cut into thin sections using an ultramicrotome (thickness of the sections <100 nm). The slices were supported on formvar/carbon film 100 mesh nikel grids. Thermogravimetric analysis (TGA) was measured by using a TGA Q500 system (TA instrument) with a heating rate of 10°C min^{-1} under nitrogen atmosphere. The ultraviolet–visible (UV–vis) transmission spectra were measured on a TU-1901 spectrophotometer. The excitation and emission spectra were carried out using a Perkinelmer LS-55 luminescence spectrometer with

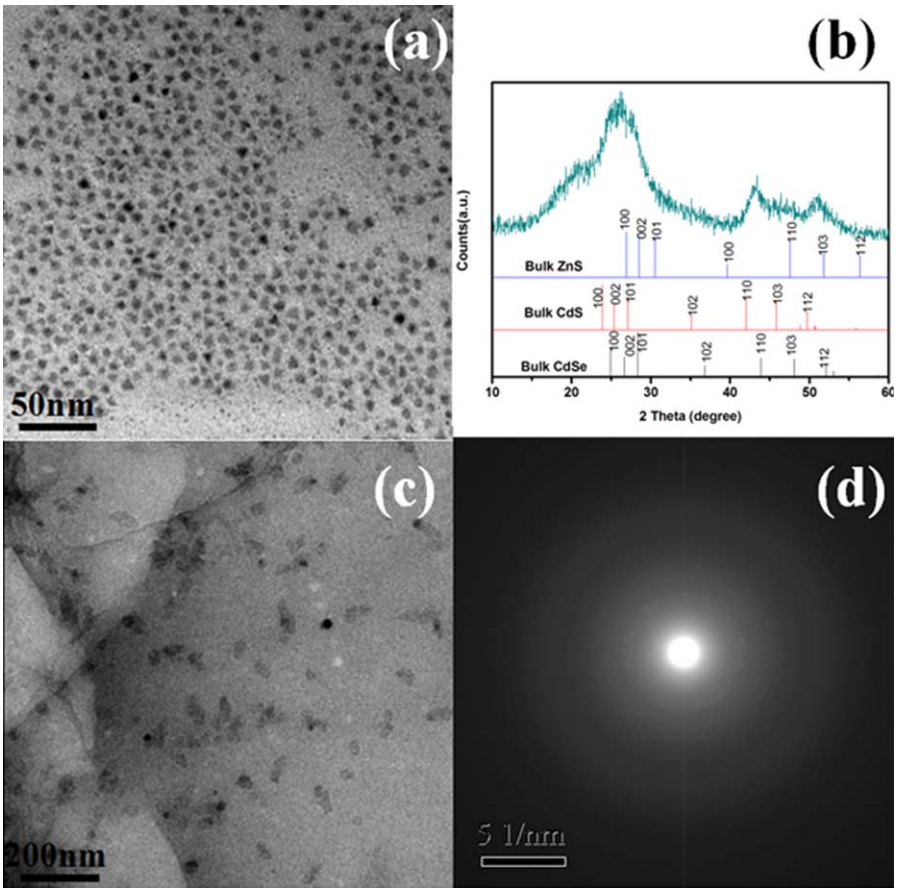

Figure 1. (a) TEM images of OA coated multilayer QDs in $CHCl_3$, (b) the XRD patterns of multilayer QDs, (c) TEM images of the multilayer QDs/PMMA nanocomposite (6 wt % multilayer QDs ultramicrotome cut, (d) the SAED pattern of multilayer QDs in PMMA. [Color figure can be viewed in the online issue, which is available at wileyonlinelibrary.com.]

a xenon lamp as an excitation source at room temperature. The X-ray excited luminescence (XL) spectra were measured by X-ray excited spectrometer, Fluor Main, where an F-30 X-ray tube (W anticathode target) was used as the X-ray source, and operated under 80 kV and 6 mA.

RESULTS AND DISCUSSION

Characterization of Core/Multishell QDs

Core/multishell CdSe/CdS/CdS/$Cd_{0.75}Zn_{0.25}S$/$Cd_{0.5}Zn_{0.5}S$/$Cd_{0.25}Zn_{0.75}S$/ZnS/ZnS nanocrystals were obtained according to a previously reported protocols via successive ion layer adsorption and reaction (SILAR) using the convention nonhydrolytic solvent method. Our previous results show that the CdSe/CdS/CdS/$Cd_{0.75}Zn_{0.25}S$/$Cd_{0.5}Zn_{0.5}S$/$Cd_{0.25}Zn_{0.75}S$/ZnS/ZnS nanocrystals have good stability and relative high quantum yield (47.8%).[9] The morphology and structure of as-prepared QDs are characterized by TEM and XRD [Figure 1(a,b)].The as-prepared QDs are uniform with average size about 10 nm, as seen from Figure 1(a). The X-ray diffraction pattern was almost the same as ZnS nanocrystals of the same size due to the most fraction ZnS took up [Figure 1(b)], which is similar to the reported results of Ref. [40] The crystal domain size calculated using the Scherrer equation with the (103) peak is about 10 nm, which is consistent with the TEM result in Figure 1(b).

Surface Modification of Core/Multishell QDs

To generate homogeneous and transparent nanocomposite, it is necessary to transfer the nanocrystals into monomer solution to form to a stable dispersion. However, OA coated particles cannot be directly dispersed in MMA without severe agglomeration, which leads to an unstable and opaque dispersion [Figure 1(a)]. In our approach, the particles were modified with PEG-oleate, resulting in a stable and transparent dispersion of the nanosized particles in MMA, as showed in Figure 1(b). The surfactant of amphiphilic polymer PEG-oleate has a long chain alkyl at one end interacting with the surface of QDs while PEG chains at the other end which is compatible with MMA monomer. The interdigitation of the PEG-oleate with the oleic acid on the surface of the QDs rendered the QDs dispersible in MMA. In fact, the transparent solution can even maintain for several months.

The Preparation of Core/Multishell QDs/PMMA Nanocomposites

A stable dispersion does not always lead to transparent nanocomposites due to polymerization of the monomer dispersion can lead to phase separation of the QDs and agglomeration, leading to inhomogeneity and luminescence quenching.[30,36] Zhang et al.[30] utilized polymerizable surfactants instead of nonpolymerization surfactants to successfully prevent phase separation during

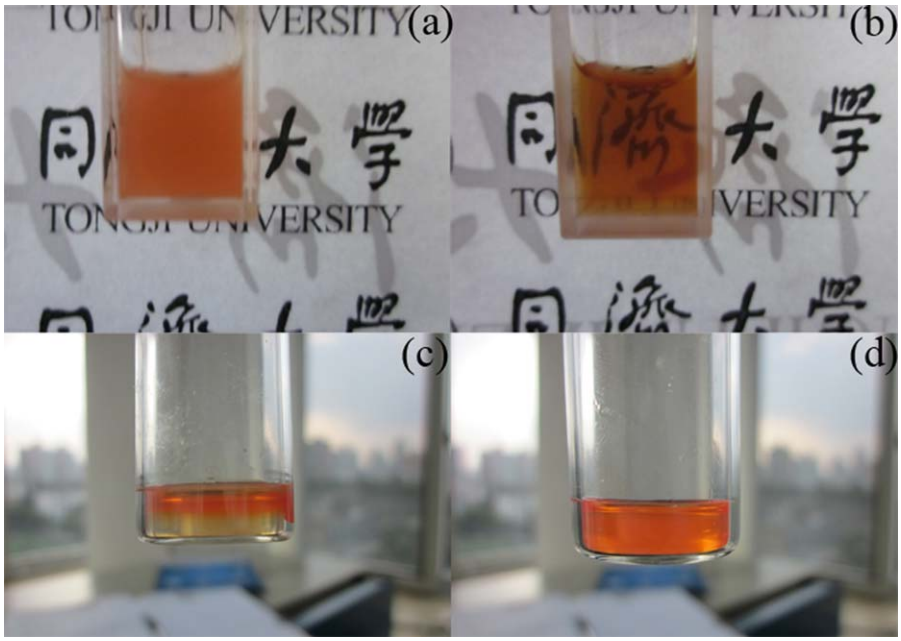

Figure 2. (a) Photographs of OA coated QDs in MMA, (b) amphiphilic polymer PEG-oleate modified QDs in MMA, (c) OA-PEG modified QDs in PMMA resin obtained through thermalpolymerization, (d) through photopolymerization. [Color figure can be viewed in the online issue, which is available at wileyonlinelibrary.com.]

polymerization. In our approach, a transparent and homogeneous bulk nanocomposite was obtained by photopolymerizaion [Figure 1(d)]. While we initiated the polymerization by heating, almost all the QDs moved to the top of the substrate [Figure 1(c)]. The possible reason maybe as follows: the PEG-oleate capped QDs dissolve in MMA easier than in polymerized PMMA owing to the difference in the viscosity, for thermal polymerization, it usually takes a long time to completely polymerize, when MMA is polymerized to PMMA, the large molecular mass PMMA sinks to the bottom, leaving the QDs on the upper section of the sample.[20] In contrast, the transparent and homogenous bulk nanocomposite was successfully obtained by proposed photopolymerization approach, as shown in Figure 1(d). It is clear that photopolymerization of all sections are initiated at the same time, moreover, photopolymerization rate is rapid enough to complete the polymerization before PMMA sinking down from the MMA, so our proposed approach seems more facile to achieve.

The Characterization of Core/Multishell QDs/PMMA Nanocomposites

A representative TEM of the nanocomposite with the content of 6 wt % QDs is shown in Figure 1(c) (ultramicrotome cut, thickness 50–70 nm). From the image it can be seen that the QDs are well dispersed in PMMA with only a few nanoparticles agglomeration. Most of the agglomerations are below 20 nm, consisting of only two to three QDs, which contributes to the transparence of the nanocomposites. The lattice parameters derived from selected-area electron diffraction (SAED) of QDs in composites are consistent with zinc blende structure, matching well with XRD pattern of multilayer QDs, which further confirms the existence of QDs in PMMA matrix [Figure 1(d)].

Figure 2 shows the transmittance spectra of QDs/PMMA nanocomposites with various amounts of QDs. The pure PMMA has a transmittance of 89% across the range of 600–800 nm [Figure 2(a)]. The loss of 11% is caused by reflection on the two surfaces of the block (2 mm thickness). With the increasing of the QDs contents from 3 to 6 wt %, just a little drop of transmittance is observed [Figure 2(b–d)]. The transmittance of composites with the content of 6 wt % QDs is still as high as 82% in the range of 600–800 nm. The inset of Figure 2 shows the photographs of QDs/PMMA nanocomposites filled with various QDs contents under ambient light. The clear samples are also correspondent with results of the transmittance spectra.

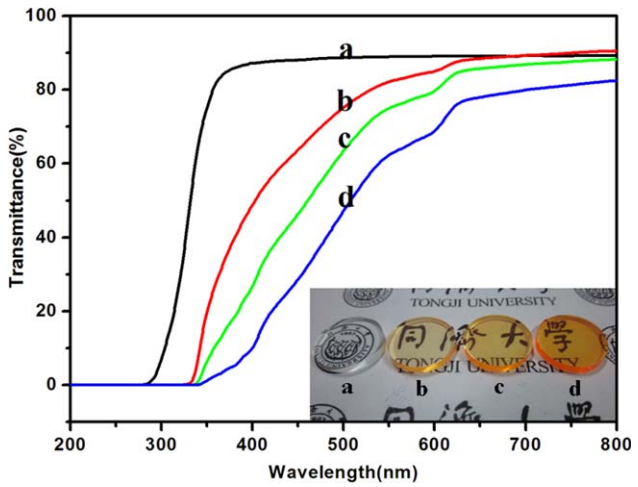

Figure 3. (a) Transmission spectra of pure PMMA and QDs/PMMA nanocomposites with the QDs content of (b) 3 wt %, (c) 4 wt %, (d) 6 wt %, respectively. The inset shows the photograph of corresponding samples under ambient light. All the samples are in sizes with φ 15.7 mm × 2.2 mm. [Color figure can be viewed in the online issue, which is available at wileyonlinelibrary.com.]

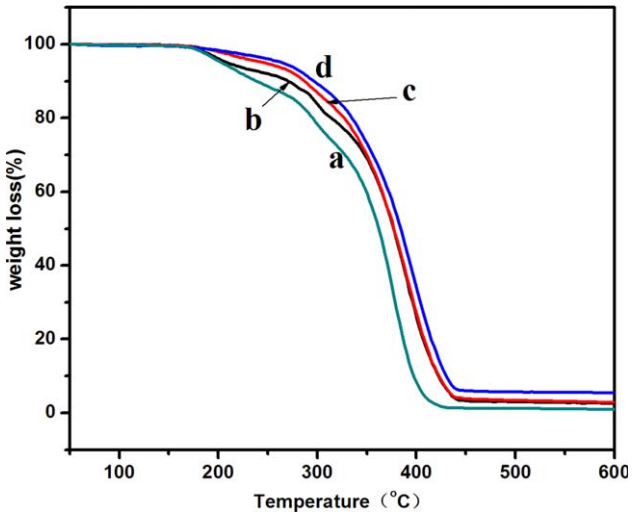

Figure 4. (a) TGA curves of pure PMMA, QDs-PMMA nanocomposites with the QDs content of (b) 3 wt %, (c) 4 wt %, and (d) 6 wt %, respectively. [Color figure can be viewed in the online issue, which is available at wileyonlinelibrary.com.]

The thermal stability of the nanocomposites was investigated with themogravimetric analysis (TGA). As shown in Figure 3, the pure PMMA [Figure 3(a)] started to decompose at about 197°C (here the decomposition temperature is defined as 2% weight loss of samples[41], while the nanocomposites with the incorporation of 3, 4, and 6 wt % QDs began to decompose at 195, 227, and 257°C, respectively. It is clear that the decomposition temperature increases with the increase of QDs contents, the degradation initiation of nanocomposite with 6 wt % QDs content even retard by 60°C.The improvement in the thermal property of the QDs/PMMA nanocomposites could be attributed to the increase of the interface between the QDs and polymer and the interaction between the surface of QDs and the polymer chains. The further crosslinking in the QDs/PMMA nanocomposite blocks hindered the movement of PMMA strand and prevented its thermal decomposition.[41,42] The residues of b, c, d nanocomposites at 600°C obtained from TGA results are 2.5, 2.8, and 5.5 wt %, respectively, which are by and large in accordance with the calculate values of pure QDs weight contents of QDs in the nanocomposites.

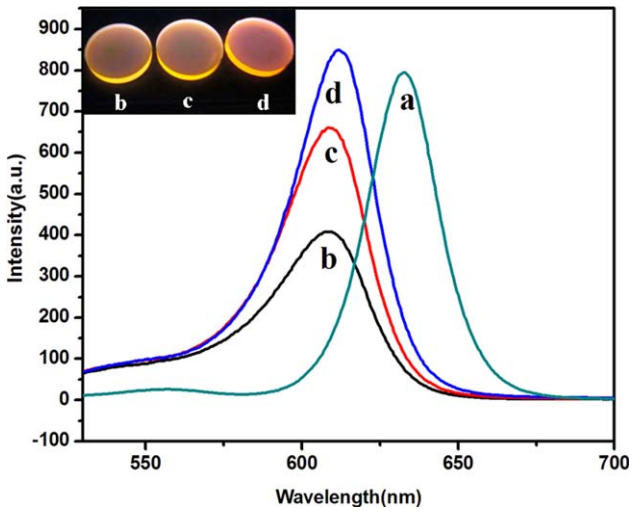

Figure 5. (a) PL spectra of QDs in $CHCl_3$ and QDs/PMMA nanocomposites with the QDs content (b) 3 wt %, (c) 4 wt %, (d) and 6 wt %. PL spectra were recorded with an excitation at 365 nm. The inset shows the photograph of corresponding samples under 365-nm excitation in dark. [Color figure can be viewed in the online issue, which is available at wileyonlinelibrary.com.]

Figure 4 shows the PL spectra of colloidal solutions of QDs in $CHCl_3$ and QDs/PMMA nanocomposites with various amounts of QDs. Through all processing steps, the optical properties of the core/multishell QDs are mainly retained with slight change. Under the excitation of 365 nm, the PL emission peaks of QDs/PMMA nanocomposites are all blue-shifted (608–611 nm) compared with the corresponding peaks in chloroform (632 nm). Blue shift of PL spectra is also observed in other QDs/polymer nanocomposites and attributed to the oxidation of the QDs surface.[20,43] For our case, the situation seems similar. During the photopolymerization, the ultraviolet radiation may oxidize the QDs surface, reducing the QDs size and causing the blue shift of PL peak wavelength due to the quantum size effect.[44] The inset of Figure 4 shows photograph of QDs/PMMA bulk nanocomposites with different QDs content under 365 nm excitation in dark, demonstrating a bright orange emission from the nanocomposites.

Figure 5 shows the emission spectra recorded under X-ray excitation at room temperature for QDs/PMMA nanocomposites with 6 wt % QDs. The X-ray excited emission spectra of the nanocomposite present a shape peak emission at 611 nm corresponding to interband excitonic transition of QDs, which is in line with its PL spectra shown in Figure 4. This indicates that the as-prepared naocomposites have the potential application for X-ray detection.

CONCLUSION

We have developed an efficient and facile method to prepare core/multishell QDs/PMMA bulk nanocomposites. Amphiphilic polymer PEG-oleate was used to stabilize the QDs in MMA monomer. Photopolymerization could successfully prevent the phase separation during polymerization, which results in the

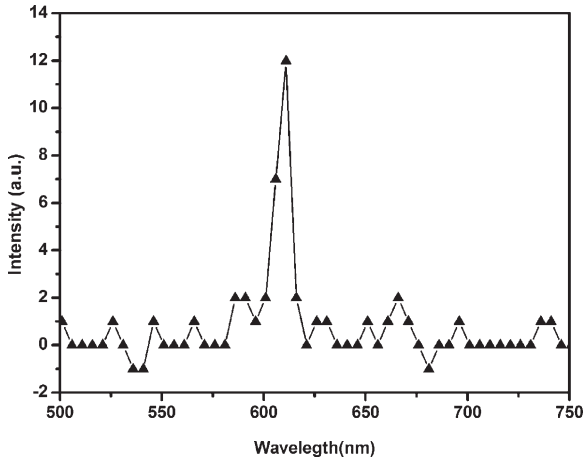

Figure 6. Emission spectra of QDs/PMMA nanocomposites with 6 wt % QDs under X-ray excitation.

production of transparent and homogenous core/multishell QDs/PMMA bulk nanocomposites with QDs contents of 6 wt %. Under UV excitation, the composites show bright luminescence and a blue-shift of the emission peak is observed with respect to that in $CHCl_3$, which may be related to the alteration of dielectric environment. The bright PL emission and improved thermal stability imply that the investigated core/multishell QDs/PMMA nanocomposites have potential applications for optical communication devices and radiation detectors.

ACKNOWLEDGMENTS

This work is supported by National Natural Science Foundation of China (Grant No. 10904114, No. 91022002 and No. 10974143), Significant National Special Project of the Ministry of Science and Technology of China for Development of Scientific Instruments and Equipment (Grant no. 2011YQ13001902), and the Program for Young Excellent Talents in Tongji University (2009KJ072), and the Fundamental Research Funds for the Central Universities. The authors are grateful to Dr. F. C. J. M. van Veggel at University of Victoria (Canada) and Hao Zhang at Jilin University (China) for helpful discussions.

REFERENCES

1. Alivisatos, A. P. *Science* **1996**, *271*, 933.
2. Tang, Z.; Kotov, N. A.; Giersig, M. *Science* **2002**, *297*, 237.
3. Colvin, V. L.; Schlamp, M. C.; Alivisatos, A. P. *Nature* **1994**, *370*, 354.
4. Sundar, V. C.; Eisler, H. J.; Bawendi, M. G. *Adv. Mater.* **2002**, *14*, 739.
5. Bruchez, M., Jr.; Moronne, M.; Gin, P.; Weiss, S.; Alivisatos, A. P. *Science* **1998**, *281*, 2013.
6. Letant, S. E.; Wang, T. F. *Nano Lett.* **2006**, *6*, 2877.
7. Campbell, I. H.; Crone, B. K. *Adv. Mater.* **2006**, *18*, 77.
8. Kang, Z. T.; Zhang, Y. L.; Menkara, H.; Wagner, B. K.; Summers, C. J.; Lawrence, W.; Nagarkar, V. *Appl. Phys. Lett.* **2011**, *98*, 181914.
9. Zhang, B.; Chen, B.; Wang, Y.; Guo, F.; Li, Z.; Shi, D. J. *Colloid Interface Sci.* **2011**, *353*, 426.
10. Zhang, B.; Gong, X.; Hao, L.; Cheng, J.; Han, Y.; Chang, J. *Nanotechnology* **2008**, *19*, 465604.
11. Zhang, B.; Cheng, J.; Gong, X.; Dong, X.; Liu, X.; Ma, G.; Chang, J. *Colloid Interface Sci.* **2008**, *322*, 485.
12. Tomczak, N.; Janczewski, D.; Han, M. Y.; Vancso, G. J. *Prog. Polym. Sci.* **2009**, *34*, 393.
13. Li, S.; Lin, M. M.; Toprak, M. S.; Kim, D. K.; Muhammed, M. *Nano Rev.* **2010**, *1*, 1.
14. Zhang, H.; Han, J.; Yang, B. *Adv. Func. Mater.* **2010**, *20*, 1533.
15. Striccoli, M.; Tamborra, M.; Comparelli, R.; Curri, M. L.; Petrella, A.; Agostiano, A. *Nanotechnology* **2004**, *15*, S240.
16. Wang, W. Y.; Liu, J.; Yu, X. B.; Yang, G. Q. *J. Nanosci. Nanotechnol.* **2010**, *10*, 5196.
17. Song, H.; Lee, S. *Nanotechnology* **2007**, *18*, 055402.
18. Sardar, D. K.; Chandra, S.; Gruber, J. B.; Gorski, W.; Zhang, M. G.; Shim, J. H. *J. Appl. Phys.* **2009**, *105*, 093105.
19. Tan, M. C.; Patil, S. D.; Riman, R. E. *Acs Appl. Mater. Inter.* **2010**, *2*, 1884.
20. Pang, L.; Shen, Y. M.; Tetz, K.; Fainman, Y. *Opt. Express* **2005**, *13*, 44.
21. Zhen, Z.; Wang, J. S.; Hu, J.; Tang, D. H.; Liu, X. H. *J. Mater. Chem.* **2007**, *17*, 1597.
22. Boyer, J. C.; Johnson, N. J. J.; van Veggel, F. C. J. M. *Chem. Mater.* **2009**, *21*, 2010.
23. Chai, R. T.; Lian, H. Z.; Yang, P. P.; Fan, Y.; Hou, Z. Y.; Kang, X. J.; Lin, J. *J. Colloid Interface. Sci.* **2009**, *336*, 46.
24. Andrews, P. C.; Brown, D. H.; Fraser, B. H.; Gorham, N. T.; Junk, P. C.; Massi, M.; St Pierre, T. G.; Skelton, B. W.; Woodward, R. C. *Dalton T.* **2010**, *39*, 11227.
25. Mamedov, A. A.; Belov, A.; Giersig, M.; Mamedova, N. N.; Kotov, N. A. *J. Am. Chem. Soc.* **2001**, *123*, 7738.
26. Gao, M.; Sun, J.; Dulkeith, E.; Gaponik, N.; Lemmer, U.; Feldmann, J. *Langmuir* **2002**, *18*, 4098.
27. Jin, Y. Z.; Tu, Y.; Zhou, L.; Gao, C.; Ye, Z. Z.; Yang, Y. F.; Wang, Q. L. *J. Mater. Chem.* **2010**, *20*, 1594.
28. Guan, C.; Lu, C.; Cheng, Y.; Song, S.; Yang, B. *J. Mater. Chem.* **2009**, *19*, 617.
29. Shen, H. X.; Chen, L.; Chen, S. J. *Inorg. Organomet. Polym. Mater.* **2009**, *19*, 374.
30. Zhang, H.; Cui, Z.; Wang, Y.; Zhang, K.; Ji, X.; Lü, C.; Yang, B.; Gao, M. *Adv. Mater.* **2003**, *15*, 777.
31. Althues, H.; Palkovits, R.; Rumplecker, A.; Simon, P.; Sigle, W.; Bredol, M.; Kynast, U.; Kaskel, S. *Chem. Mater.* **2006**, *18*, 1068.
32. Chen, L.; Zhu, J.; Li, Q.; Chen, S.; Wang, Y. *Eur. Polym. J.* **2007**, *43*, 4593.
33. Erskine, L.; Emrick, T.; Alivisatos, A.; Frechet, J. *Polym. Polym. Prepr.* **2000**, *41*, 593.
34. Zhang, H.; Wang, C.; Li, M.; Ji, X.; Zhang, J.; Yang, B. *Chem. Mater.* **2005**, *17*, 4783.
35. Woelfle, C.; Claus, R. O. *Nanotechnology* **2007**, *18*, 025402.
36. Lee, J.; Sundar, V. C.; Heine, J. R.; Bawendi, M. G.; Jensen, K. F. *Adv. Mater.* **2000**, *12*, 1102.
37. Peng, X. G. *Adv. Mater.* **2003**, *15*, 459.
38. Wang, X. B.; Li, W. W.; Sun, K. *J. Mater. Chem.* **2011**, *21*, 8558.
39. Anseth, K. S.; Wang, C. M.; Bowman, C. N. *Polymer* **1994**, *35*, 3243.
40. Li, J. J.; Wang, Y. A.; Guo, W. Z.; Keay, J. C.; Mishima, T. D.; Johnson, M. B.; Peng, X. G. *J. Am. Chem. Soc.* **2003**, *125*, 12567.
41. Zeng, X. F.; Kong, X. R.; Ge, J. L.; Liu, H. T.; Gao, C.; Shen, Z. G.; Chen, J. F. *Ind. Eng. Chem. Res.* **2011**, *50*, 3253.
42. Aymonier, C.; Bortzmeyer, D.; Thomann, R.; Mülhaupt, R. *Chem. Mater.* **2003**, *15*, 4874.
43. Cheng, C.; Wang, S.; Cheng, X. *Opt. Laser Technol.* **2012**, *44*, 1298.
44. Nazzal, A. Y.; Wang, X. Y.; Qu, L. H.; Yu, W.; Wang, Y. J.; Peng, X. G.; Xiao, M. J. *Phys. Chem. B* **2004**, *108*, 5507.